反应等离子熔敷原位合成高铬铁基复合涂层高温抗氧化性

王立梅

（潍坊学院 信息与控制工程学院，山东 潍坊 261061）

摘 要：利用前驱体碳化复合粉末制备技术，以蔗糖为碳的前驱体，制备了反应等离子熔敷 Fe-Cr-C-W-Ni 复合粉末；采用优化的反应等离子熔敷工艺，在调质 C 级钢（C≤0.35%）基材表面制备了以原位生成初生相 $(Cr, Fe)_7C_3$ 为增强相，以 γ 固溶体与少量 $(Cr, Fe)_7C_3$ 构成的共晶为基体的高铬铁基金属陶瓷复合涂层．应用 EDS，SEM，XRD 等研究了涂层的成分和组织结构．在900 ℃恒温氧化50 h的试验条件下测试了涂层的抗氧化性及氧化动力学曲线．结果表明，复合材料涂层及氧化膜的显微组织结构和相组成主要包括 Cr_2O_3 和 Fe_2O_3，涂层具有较好抗氧化性能的原因是连续致密的氧化膜 Cr_2O_3 和 Fe_2O_3 阻挡了涂层被进一步氧化．

关键词：反应等离子熔敷；高铬铁基复合涂层；前驱体；显微组织；抗氧化性

中图分类号：TG115 文献标识码：A 文章编号：0253－360X(2009)01－0093－03

王立梅

0 序 言

反应熔敷技术是在激光或等离子等高能量束熔敷过程中通过元素或化合物间的化学反应“原位合成”金属陶瓷等涂层的一种新型涂层技术．近年来，反应熔敷技术受到了国内外的普遍关注[1－4]．等离子熔敷技术与激光熔敷技术相比较，具有能量转换效率高、设备投资小、操作维修简便等特点[5]．金属碳化物 $(Cr, Fe)_7C_3$ 具有熔点高、高温硬度高、高温稳定性好、高温抗氧化性能优异且在高温下具有较高韧性等特点，但严重的室温脆性是目前作为整体材料使用的主要障碍之一．然而 $(Cr, Fe)_7C_3$ 金属陶瓷具有硬度高、耐腐蚀性及抗氧化性好等优点，常被用作耐磨或抗氧化涂层的增强相[6,7]．

作者利用前驱体碳化复合粉末制备技术，以蔗糖为碳的前驱体，制备了反应等离子熔敷 Fe-Cr-C-W-Ni 复合粉末．采用同步送粉反应等离子熔敷设备和优化的反应等离子熔敷工艺，在调质C级钢（C≤0.35%）基材表面制备了以原位生成初生相 $(Cr, Fe)_7C_3$ 为增强相，以 γ 固溶体与少量 $(Cr, Fe)_7C_3$ 构成的共晶为基体的高铬铁基金属陶瓷复合涂层．在900 ℃、恒温氧化 50 h 条件下对涂层的抗氧化性进行了测试，并分析了氧化机理．

1 试验方法

以蔗糖为碳的前驱体，将其与一定量的 Fe，Cr，W，Ni 元素粉末均匀混合后置入碳化炉中．在一定温度和惰性气氛的保护下使附着在 Fe，Cr，W，Ni 元素粉末表面的蔗糖发生碳化过程，碳化所得混合物经破碎、筛分后即可获得符合熔敷粒度要求的反应熔敷复合粉末．这种复合粉末的最大特点是单质碳在一定温度下与 Fe，Cr，W，Ni 元素粉末表面经碳化反应生成，与 Fe，Cr，W，Ni 元素粉末粘结强度高，在熔敷过程中不易分离，有望解决目前反应等离子熔敷制备耐磨涂层时的反应熔敷粉末分离问题，提高涂层的质量．工艺研究表明，在 550 ℃温度下碳化，可以获得优质的 Fe-Cr-C-W-Ni 复合粉末，经破碎、筛分后取粒度大致在－200～＋300目左右的粉末．熔敷设备采用 DRF －2 型全自动反应等离子熔敷机床．以涂层与基材表面的结合性能及基材对涂层成分的稀释率为指标，试验确定了前驱体碳化复合粉末反应等离子熔敷的最佳工艺参数分别为工作电流 300 A，工作电压 30 V，送粉量 30 g/min，扫描速度

收稿日期：2007－12－18
基金项目：山东省科技攻关项目(2007GG30003003)

500 mm/min, 工作气(Ar)流量 2.5 L/min, 送粉气(Ar)流量 3 L/min.

等离子熔敷基材为调质 C 级钢(C≤0.35%), 试样尺寸为 50 mm×20 mm×10 mm. 用 JSM —5800 型扫描电子显微镜观察涂层显微组织及氧化膜表面组织, 采用日本理学 Dmax —2200pc 旋转阳极 X 射线衍射仪并结合 S —530 型 LinkISIS 能谱仪进行物相鉴定, 利用线切割机将等离子熔敷复合材料涂层由基体上切下, 并切割成尺寸为 10 mm×10 mm×1 mm 的片状氧化试样, 试样的 10 mm×10 mm 表面要经磨削加工, 以避免进行尺寸测量时产生过大误差. 恒温氧化试验在高温空气电阻炉中进行, 试验温度为 900 ℃, 氧化时间为 50 h. 氧化试验前试样用丙酮清洗, 用螺旋测微器测量试样尺寸, 并计算出总表面积, 利用准确度为 0.1 mg 的 Startorius BS 110s 型电子天平称取氧化增重.

2 试验结果与分析

2.1 复合材料涂层的显微组织

图 1 为反应等离子熔敷高铬铁基复合涂层的 XRD 分析结果. 可见, 涂层的主要组成相为 $(Cr,Fe)_7C_3$ 及 γ 固溶体. 图 2a 为涂层的典型组织形貌, 可明显看出, 涂层显微组织结构特征为黑色块状初生相均匀分布于灰白色共晶基体上. 共晶组织细小均匀, XRD 结合 EDS 分析结果表明, 规则块状初生相为 $(Cr,Fe)_7C_3$, 其体积分数约占整个涂层的 60%, 共晶基体中体积分数较高的白色组织为 γ-Fe 固溶体. EDS 分析结果表明, γ 固溶体中固溶有大量的 Cr 元素和少量的 W, Ni 元素, 在随后的冶金熔池冷却过程中以 γ 的形式保持到室温. 共晶基体中颜色较深的不规则粒状组织为共晶 $(Cr,Fe)_7C_3/\gamma$. 涂层与基材结合区部位(图 2b)的 C 级钢基材在熔敷过程中固溶了大量的 Cr 元素和少量的 W, Ni 元素, C 级钢基材上的 γ 固溶体树枝晶由基材外延生长至熔敷涂层内部, 可见, 熔敷涂层与基材之间形成了良好的冶金结合.

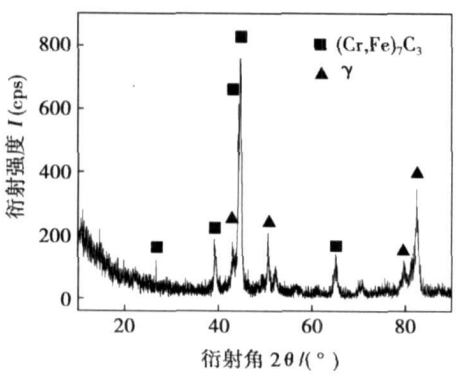

图 1 反应等离子熔敷高铬铁基复合涂层 X 射线衍射结果

Fig. 1 XRD pattern of high-chromium iron-base composite coating in reactive plasma cladding

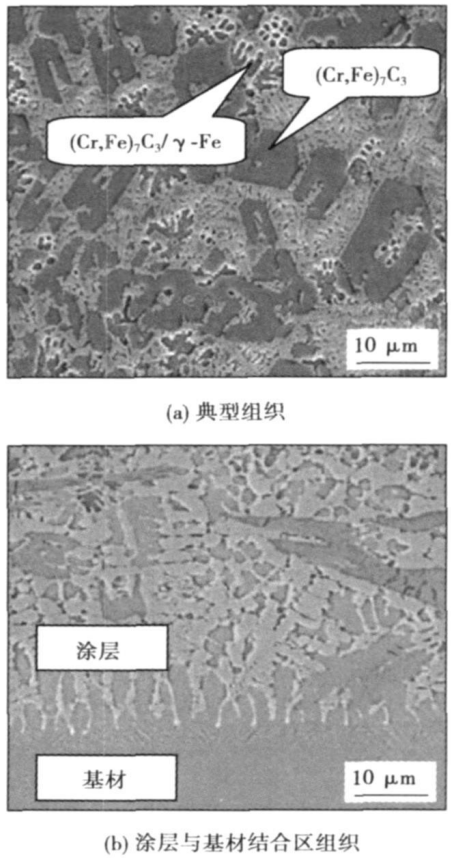

图 2 复合涂层 SEM 形貌

Fig. 2 SEM micrographs of composite coating

2.2 复合涂层的抗氧化性

图 3 为调质 C 级钢(图 3a)和反应等离子熔敷原位合成高铬铁基复合材料涂层(图 3b)经 900 ℃恒温氧化 50 h 后氧化膜的表面形貌. 明显可见, 调质 C 级钢的氧化表面氧化膜疏松、致密性差, 强度很低, 有明显的裂纹及孔洞. 而反应等离子熔敷涂层氧化膜致密、强度高, 表面无明显的裂纹及孔洞. 二者相比之下, 涂层明显具有较好的高温抗氧化性, 与未经熔敷的调质 C 级钢相比, 抗氧化性提高了 2.1 倍. 涂层的氧化动力学曲线近似符合抛物线规律(图 4), 说明氧化受扩散控制.

反应等离子熔敷原位合成高铬铁基复合材料涂层经 900 ℃高温氧化 10 h 后氧化膜的 XRD 分析结果如图 5 所示. 可见, 氧化膜的主要组成相为 Cr_2O_3 和 Fe_2O_3. 结合 EDS 分析结果表明, 白色不规则组织为 Cr_2O_3, 灰色粒状组织为 Fe_2O_3(图 3b). 由于涂层

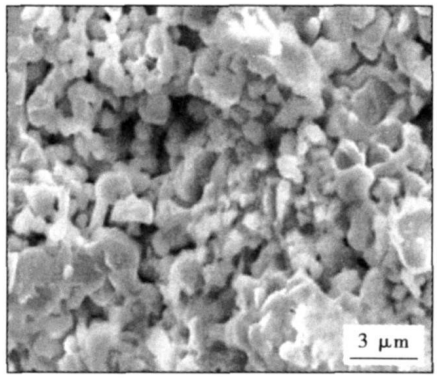

(a) 调质C级钢

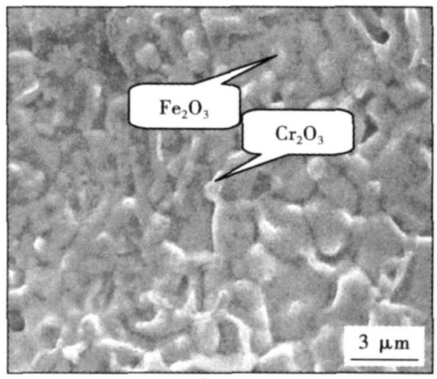

(b) 涂层

图 3　氧化膜表面形貌

Fig. 3　SEM micrographs of oxide film surface

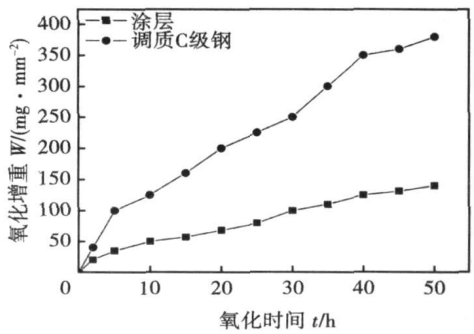

图 4　复合涂层的氧化动力学曲线

Fig. 4　Oxidation kinetics of composite coating

中含有大量 Cr 元素的同时还固溶有少量来自基材的 Fe 元素,在氧化反应初期,以 Cr 元素向外扩散为主. 由于 Cr 元素的扩散速度很快,因此 Cr 元素的氧化物向外生长并迅速长大,在最外面形成了 Cr_2O_3 层. 氧化物的形成使 Fe 元素得到富集,又促进了 Fe 元素的的氧化物的形成,于是在表面 Cr_2O_3 层以下形成了较致密的 Cr_2O_3 和 Fe_2O_3 的混合层. 这层混合阻挡层的存在,降低了氧化过程的氧化速率,在随后的氧化过程中 Cr 元素的向外扩散和氧的向内扩散同时起了作用. Cr 元素向外扩散在氧化物/空气界面形成了 Cr_2O_3 层,氧向内扩散的结果形成了里面的 Cr_2O_3 和 Fe_2O_3 的混合层,混合层相对致密. 混合层的形成阻碍了氧向内扩散,使氧化层下的氧分压降低,避免了涂层进一步被氧化,这也是涂层具有较好抗氧化性的一个原因. 在氧化的初期,Cr_2O_3 在金属与氧化层界面形核,先垂直于基体生长,然后再横向相连生长,这种生长方式使得氧化层与基体的界面存在着许多大的孔洞. 孔洞的形成减弱了氧化膜与基体之间的结合力,同时使氧化过程中产生的应力不断得到松弛,避免了氧化膜整体脱落. 图 6 为氧化膜横截面 SEM 形貌. 可见氧化膜表面及横截面质量较好,氧化膜连续、致密、均匀、无裂纹及孔洞. 连续致密的氧化膜层,弥散分布着具有良好保护作用的 Cr_2O_3 和 Fe_2O_3,对于抑制金属离子及氧离子的扩散起到了重要作用,这是涂层与调质 C 级钢相比具有较好抗氧化性的主要原因.

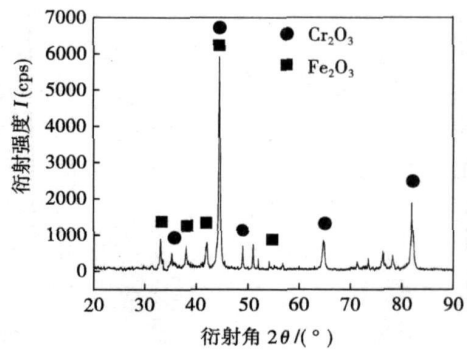

图 5　复合涂层氧化膜 X 射线衍射图谱

Fig. 5　XRD pattern of oxide film of composite coating

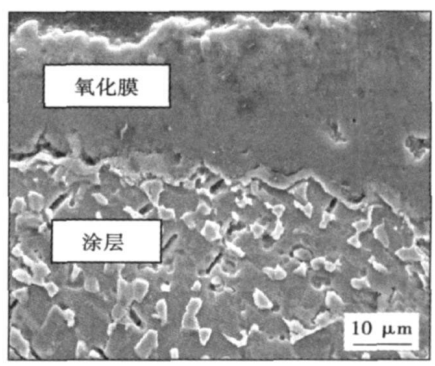

图 6　涂层氧化膜横截面 SEM 形貌

Fig. 6　SEM micrograph of oxide film cross-section

[下转第 104 页]

参考文献：

[1] 国旭明，钱百年，张 艳，等. 外场处理细化管线钢埋弧焊缝的显微组织[J]. 焊接学报，2001，22(2)：27－30.
Guo Xuming，Qian Bainian，Zhang Yan，*et al*. Refining microstructure of submerged arc weld metal by using outer field treatment[J]. Transactions of the China Welding Institution，2001，22(2)：27－30.

[2] 周振丰. 焊接冶金学[M]. 北京：机械工业出版社，1995.

[3] Tao N R，Wang Z B，Tong W P，*et al*. An investigation of surface nanocrystallization mechanism in Fe induced by surface mechanical attrition treatment[J]. Acta Materialia，2002，50(18)：4603－4616.

[4] Mordyuk B N，Prokopenko G I. Fatigue life improvement of α-titanium by novel ultrasonically assisted technique[J]. Materials Science and Engineering A，2006，A437(2)：396－405.

[5] 王东坡，霍立兴，张玉凤，等. 提高焊接接头疲劳强度的超声冲击法. 焊接学报[J]. 1999，20(3)：158－163.
Wang Dongpo，Huo Lixing，Zhang Yufeng，*et al*. Enhanced fatigue strength of welded joints by means of ultrasonic impact technique[J]. Transactions of the China Welding Institution，1999，20(3)：158－163.

[6] Minoru Furukawa，Zenji Horita，Minoru Nemoto，*et al*. The use of severe plastic deformation for microstructural control[J]. Materials Science and Engineering A，2002，324(1－2)：82－89.

[7] Ohsaki S，Kato S，Tsuji N，*et al*. An investigation of surface nanocrystallization mechanism in Fe induced by surface mechanical attrition treatment[J]. Acta Materialia，2007，55(8)：2885－2895.

[8] Shankar M Ravi，Rao Balkrishma C，Lee Seongeyl，*et al*. Severe plastic deformation (SPD) of titanium at near-ambient temperature [J]. Acta Materialia，2006，54(14)：3691－3700.

[9] Liu G，Wang S C，Lou X F，*et al*. Low carbon steel with nanostructured surface layer induced by high-energy shot peening[J]. Scripta Materialia，2001，44(8－9)：1791－1795.

[10] 李 东，陈怀宁，刘 刚，等. SS400 钢焊接接头表层组织纳米均一化及硬度均一化处理[J]. 金属学报，2001，37(9)：981－984.
Li Dong，Chen Huaining，Liu Gang，*et al*. Homogenization of microstructure and hardness of surface layer of SS400 steel welded joints [J]. Acta Metallurgica Sinica，2001，37(9)：981－984.

作者简介：李 东，男，1974 年出生，博士. 主要从事纳米材料及材料表面改性方面的研究. 发表论文 10 余篇.

Email：dli@ecust.edu.cn；freedomsli@yahoo.com

[上接第 95 页]

3 结 论

(1) 利用前驱体碳化复合粉末制备技术，以蔗糖为碳的前驱体，制备了反应等离子熔敷 Fe-Cr-C-W-Ni 复合粉末.

(2) 采用同步送粉反应等离子熔敷设备和优化的反应等离子熔敷工艺，在调质 C 级钢基材表面制备了以原位生成初生相 $(Cr,Fe)_7C_3$ 为增强相，以 γ 固溶体与少量 $(Cr,Fe)_7C_3$ 构成的共晶为基体的高铬铁基金属陶瓷复合涂层. 涂层组织均匀细小，无显微孔洞和裂纹，与基材完全冶金结合.

(3) 涂层在 900 ℃高温氧化试验条件下具有良好的抗氧化性能.

参考文献：

[1] 刘均波，黄继华，王立梅. 反应等离子熔敷 Cr_7C_3/γ-Fe 金属陶瓷复合材料涂层组织与耐磨性[J]. 焊接，2005(4)：49－52.
Liu Junbo，Huang Jihua，Wang Limei. Microstructure and wear resistance of the reactive plasma clad Cr_7C_3/γ-Fe ceramal compositl coating [J]. Welding and Joining，2005(4)：49－52.

[2] 殷 声. 燃烧合成[M]. 北京：冶金工业出版社，1999.

[3] 刘均波，王立梅，黄继华，等. 离子熔覆 Cr_7C_3/γ-Fe 金属陶瓷复合材料涂层的耐磨性[J]. 机械工程材料，2006，30(2)：42－45.
Liu Junbo，Wang Limei，Huang Jihua，*et al*. Wear properties of plasma clad Cr_7C_3/γ-Fe ceramal composite coating[J]. Materials for Mechanical Engineering，2006，30(2)：42－45.

[4] 孙荣禄，杨贤金. 激光熔敷原位合成 TiC-TiB_2/Ni 基金属陶瓷涂层的组织和摩擦磨损性能[J]. 硅酸盐学报，2003，31(12)：1221－1224.
Sun Ronglu，Yang Xianjin. Microstructure friction and wear properties of in situ synthesized TiC-TiB_2/Ni-based metallic ceramic coating by laser cladding[J]. Journal of the Chinese Ceramic Society，2003，31(12)：1221－1224.

[5] Liu J B，Huang J H，Wang L M. Study on PTA clad $(Cr,Fe)_7C_3$/γ-Fe ceramal composite coating [J]. Acta Metallurgica Sinica (English letters)，2005，18(6)：695－700.

[6] Liu C T，Steigler J O，Sam F H. Metals handbook[M]. 10th Edition. USA：The Materials Information Society，USA：1990.

[7] 刘均波. 等离子表面冶金(Cr，Fe)$_7C_3$/γ-Fe 金属陶瓷复合涂层工艺[J]. 焊接学报，2007，28(4)：17－20.
Liu Junbo. Process of (Cr，Fe)$_7$C3/γ-Fe ceramal composite coating formed by plasma surface metallurgy[J]. Transactions of the China Welding Institution，2007，28(4)：17－20.

作者简介：王立梅，女，1975 年出生，在职研究生，实验师. 主要从事材料表面涂层技术和粉末冶金方面的研究和实验室管理工作. 发表论文 15 余篇.

Email：meiliwang620@163.com

Zhenjiang 212003 Jiangsu, China). p73—76

Abstract: Different from the relationship of heat input and welding speed at melting welding, which submits inverse ratio, the relation is quite complex for friction stir welding. This paper studies the relation of welding speed and heat input at aluminum alloy friction stir welding based on thermogenesis of friction and plastic deforming. The result shows that welding speed and heat input relationship is nonlinear and shows a complex shape, which means welding speed, depending on various ranges of parameter, contributes variably to heat input. When rotary speed to welding speed ratio is constant, with the increase of welding speed, heat input and the mechanical behavior of the joint decreasing is not linear. Thus, heat input should not be measured by rotary speed to welding speed ratio.

Key words: friction stir welding; welding speed; heat input

Interface microstructure and wear properties of TiC-Ni-Mo coatings prepared by in-situ fabrication of laser cladding HE Qingkun, WANG Yong, ZHAO Weimin, CHENG Yiyuan (College of Mechanical and Electronic Engineering, China Petroleum University, Dongying 257061, Shandong China). p77—80, 100

Abstract: TiC-Ni-Mo composite coating was prepared by in-situ fabrication of laser cladding. The interface microstructure and wear properties of the coating was investigated by means of EPMA, TEM and wear tests. The results show that, adding 5% Mo into the coating could improve uniformity, rigidity, wear resistance, refine TiC grains, reduce friction coefficients and exist orientation relationship: $(001)_{TiC}//(1\bar{1}1)_{\gamma\text{-}Ni}$. The rigidity and wear resistance of coating decrease with the content of 10 % Mo. There are many directional dislocations inside TiC phase and dislocation tangles inside γ-Ni-binder phase. The wear mechanism of the coating is anti-wear action of reinforcing phases. The wear morphology is short and shallow furrows.

Key words: laser cladding; in-situ fabrication; interface; wear resistance

Study on welded metal properties of high carbon cast self-shielded flux cored wire with Nb and Mo WANG Qingbao[1], BAI Bo[1], LIU Jingfeng[1], LIAN Jing[2] (1. Welding Research Institute, Central Research Institute Building & Construction, MCC, Beijing 100088, China; 2. Heilongjiang Provinoial Installation Engineering Company, Harbin 150000, China). p81—84

Abstract: The paper studied the microstructures morphology, and the discrimination in hardness and wearability of welded metal with the addition of Nb, Mo by optical microscope and SEM. The results showed that the number of primary carbide, macrohardness and wearability were increased with the increasing the contents of Nb, Mo. Nb only resulted in NbC to strength welded metal, and but this strengthen was better; Mo not only resulted in Mo_2C but also in the primary carbide and matrix, but this strengthen was weaker than that of Nb. In order to get better wear resistance and economic benefit, it should optimize the contents of alloys and strengthen both carbide and matrix.

Key word: primary carbide; strengthen; matrix; wearability

Experimental study on compression-diffusion composite connection of Cu/Al joint HONG Liling, XIN Xuanrong, ZHANG Keke, LIU Ting, WANG Wenyan (School of Materials Science and Engineering, Henan University of Science and Technology, Luoyang 471003, Henan China). p85—88

Abstracts: Cu and Al alloy were bonded by compressiong-diffusion composite connection technology. The welding technics procedure was: Cu and Al alloy be compressed firstly, then diffused on 515 ℃ for 60 min, and diffuseed 90 min again before hot-pressed. The microstructure was researched by various test methods, such as SEM, EDS, micro-hardness test, XRD and so on. The experiment results indicated that brittle compound $CuAl_2$ appeared in the interface and a new component was created between Cu &welding, which looks like a bright belt. Electric performance of joint was between Cu and Al alloy, that could be satisfied with practical application.

Key words: compression-diffusion composite connection; copper; aluminum alloy; weld

Finite element simulation of temperature field for submerged arc strip overlaying on thick plate WANG Zhifeng[1], CHEN Peiyin[1], WU Wei[1], CHEN Yan[1], ZHANG Jianmin[2], Bao Heng[2] (1. Harbin Welding Institute, Harbin, 150080, China; 2. China First Heavy Lndustries, Qiqihar 161042, Heilongjiang China). p89—92

Abstratct: A thermal source for submerged arc overlaying is designed based on its principle and heat source model of Goldak, and a fortran subroutine is compiled to implement the translation of thermal source in the FEA software MSC. MARC. Finite element simulation of temperature field of submerged arc strip overlaying on thick plate was established. The simulation results are in good accordance with the actual thermal cycle curve, which proved the model is correct.

Key words: submergen arc overlay welding; heat source model; heat source temperature field; thermal cycle curve

Oxidation resistance of reactive plasma cladding high-chromium iron-base composite coating WANG Limei (School of Information and Control Engineering, Weifang University, Weifang 261061, Shandong China). p93—95, 104

Abstract: The sucrose was used as a carbonaceous precursor to prepare composite powders of Fe-Cr-C-W-Ni by the precursor carbonization-composition process. And the powders were fused to form a high-chromium iron-base coating on the surface of hardened and tempered grade C steel (C≤0.35%) with the optimum reactive plasma cladding process. SEM, XRD and EDS were employed to

study compositions and microstructures of the coating. The oxidation resistance of the ceramal composite coating was investigated under the testing condition of 900 ℃ and 50 hours. The results indicate that the excellent oxidation resistance of the coating is mainly attributed to the relatively continuous oxide scales which mainly consist of Cr_2O_3 and Fe_2O_3, and the oxide scales can prevent the inner part of the composite coating from being further oxidized.

Key words: reactive plasma cladding; high-chromium iron-based composite coating; precursor; microstructure; oxidation resistance

Resistance spot welding microstructure proportion simulation and experiment analysis on two aluminium alloys TANG Xinxin, SHAN Ping, LUO Zhen, LUO Baofa (College of Material Science and Engineering, Tianjin Key Laboratory of Advanced Jointing Technology, Tianjin University, Tianjin 300072, China). p96—100

Abstract: AA5754 and AA6082 aluminium alloy are two kinds of aluminius alloys with different strengthen modes. In the processing of the resistance spot welding, the microstructure of the two aluminium alloys changes in different types. By two different numerical models, the microsturcture proportion in the nuggets of the two aluminium alloys was simulated and pridicted. Conpared with the experimental results, the two simulation models are effective to predict some important phenomenas in terms of the phase transformation of the nuggets. Both the simulation results and the experimental results show that there are marked different features in the phase transformation of the two kinds of aluminium alloys.

Key words: aluminium alloy; resistant spot welding; numerical simulation; welding microstructure

Fabrication and characterization of nanocrystructured surface layer of J507 weld by ultrasonic impact peening LI Dong, FAN Zhao, LIAO Libao, ZHANG Li, XU Hong (State Key Laboratory of Chemical Engineering, School of Mechanical and Power Engineering, East China University of Science and Technology, Shanghai 200237, China). p100—104

Abstract: A nanostructured surface layer was fabricated on a J507 weld metal by. ultrasonic impact peening (UIP). The refined microstructure in the top surface layer was characterized by means of X-ray diffraction and transmission electron microscopy (TEM), and the microhardness variation along the depth of the treated sample was examined. Experimental results show that, after the UIP treatment, the microstructure of the surface layer may be refined into 21.25 nm. Grains refinement involves formation of dense dislocation walls (DDWs) and dislocation tangles (DTs) in coarse grains, transformation of DDWs and DTs into subboundaries, and evolution of subboundaries to highly misoriented grain boundaries. The strengthened thickness of the layer is 100 μm after UIP treatment. The microhardness of nanocrystalline surface layer is enhanced significantly after the UIP treatment compared with that of the original sample.

Key words: J507 weld; ultrasonic impact peening; surface nanocrystallization; microhardness

Analysis on the tendency of welding hot cracks of aluminum alloy increased by longitudinal pre-tension ZHOU Guangtao[1], LIU Xuesong[1], YANG Jianguo[1], FANG Hongyuan[1,2] (1. State Key Laboratory of Advanced Welding Production Technology, Harbin Institute of Technology, Harbin 150001, China; 2. Institute of Astronautical Technology, Shenyang Institute of Aeronautical Engineer, Shenyang 110034, China). p105—108

Abstract: Numerical simulation calculation of TIG welding of thin wall aluminum cylinder by the thermo-elastic FEM has been conducted. Based on the generating of analysis model, the values and distribution at the centre of weld seam for transverse tensile stress and strain produced by pre-tension upon the solidification metal at the back of molten pool. Experiments were performed to verify the simulation results. It can be drawn that, for weld metal just solidified at the joint pre-tension load can produce transverse tensile stress, which increases the tendency of welding hot cracks. And with the increasing of pre-tension load, the transverse tensile stress increases. When the pre-tension stress is 60, 120, 150 and 210 MPa, the crack length in specimens is 5.2 mm、8.1 mm、8.9 mm and 10.6 mm, respectively. The tests results indicates the reliability of simulation results.

Key words: pre-tension; numerical simulation; residual stress; hot cracks

Effects of M-A constituent on toughness of coarse grain heat-affected zone in HSLA steels for oil tanks ZHANG Yingqiao[1], ZHANG Hanqian[1,2], LIU Weiming[1] (1. Department of Materials Science and Engineering, Shanghai Jiaotong University, Shanghai 200030, China; 2. Research Institute for Advanced Structural Steel, R&D Center, Baoshan Iron and Steel Limited Company, Shanghai 201900, China). p109—112

Abstract: Microstructure and impact toughness of CGHAZ in HSLA steels for oil tanks under high heat input (100 kJ/cm) have been investigated. Bainite is main microstructure in CGHAZ for four steels, but there is a significant difference in impact values due to different proportion of ferrite and granular bainite. Toughness values decrease with the increase of area percentage content of M-A constituents. The effects of morphology of M-A constituents on toughness have also been studied, and the harm of massive M-A constituent is more severe than that of long strip. Considering the influence of alloy elements on the formation of M-A constituents, area percentage contents of M-A constituents are predicted by the method of multiple linear regressions, which is helpful for evaluating the toughness of CGHAZ.

Key words: heat input; coarse grain heat-affected zone; M-A constituent; impact toughness